Journal of Engineering and Applied Science

RESEARCH Open Access

Microstructural analysis of iron ore samples with bitumen as a binder

Qazi Abdul Khalique Ansari[1], Hira Lal Soni[1*], Abdul Sami Channa[1], Kashif Hussain Mangi[1] and Suhaib Ansari[2]

*Correspondence: soni.hiralal@quest.edu.pk

[1] Quaid-e-Awam University of Engineering, Science and Technology, Nawabshah, Pakistan
[2] Department of Mechanical Engineering, Isra University, Hyderabad, Pakistan

Abstract

In the present investigation, the direct reduction of magnetite and hematite powder with and without 5% bitumen at various temperatures has been studied in a hydrogen atmosphere. The prepared samples were fired in the temperature range of 673–1373 K to observe the weight loss and to find the effect of the bitumen in the samples. The microstructural results show that bitumen mixed with iron ore powder exhibited a more porous structure with cracks after reduction at 773 K and 973 K respectively. At temperatures above 1073 K, the carbon present in bitumen contributed to an enhanced rate of reduction of iron oxide samples. It was observed that, the reactivity of samples was affected by the level of impurities, crystal structure, binder, and composition of the reducing agent.

Keywords: Ion ore, Bitumen binderMicrostructure, Reduction, Pellets

Graphical Abstract

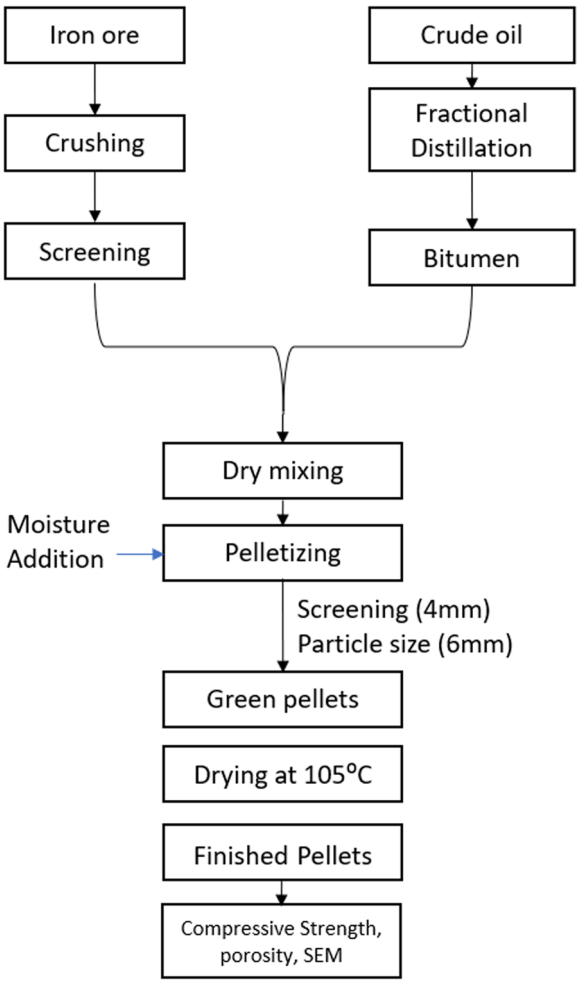

Introduction

Iron accounts for 95% of all metals used by modern industries and is closely related to the socio-economic development of the nation [1]. World reserves of iron ores are about 230 billion tons and are expected to last for more than 50 years. Around 1.73 billion tons of crude steel was produced in 2017, used in buildings, shipping, transportation, packaging and infrastructure etc [2]. The manufacturing of steel through traditional blast furnace remained the commercial method to meet the rising demand of the steel. However, during the last decade, the direct reduction has found an economic method to produce the steel without metallurgical coke and use supplement scraps as well. In direct reduction, the iron ore is not recovered as a liquid metal, as in the case when treating the material in a conventional blast furnace (indirect reduction), but as a solid product, so-called sponge iron. The sponge iron is produced from the reduction of iron ore which is further reduced to iron through pelletization with a suitable binder which imparts the green strength to the iron oxide pellets [3]. In the direct reduction, the iron-bearing charge (pellets) has to support

an optimum combination of high strength and reducibility. Studies have shown that the agglomeration of iron ore is not possible without the usage of suitable binders [4].

Over the years, metallurgical dust from steel plants is a secondary resource for a carbon-containing pellet with an appropriate binder and has become increasingly more prevalent and economic. Bentonite is universally used as a binder for iron ore pellets to improve their strength, however, it contains unwanted silica and alumina impurities that decrease the iron production rate [5]. Ripe and Kawatra found that high carbon fly ash can be used as a binder with calcium hydroxide as an activator to produce pellets of acceptable strength [6]. Utilization of serval organic and inorganic binders, such as carboxymethylcellulose (CMC), calcined colemanite, Peridur C-10, Peridur CX3, corn starch, modified starch, paper sludge, lactose monohydrate (dairy waste), and DPEP06-0007 polymer sodium lignosulfonate, has been also reported in the literature [7].

The reduction reactions of iron oxide with hydrogen (H_2) take place in the following steps:

$$\text{Hematite} - \text{magnetite}\ \ 3Fe_2O_3 + H_2 \leftrightharpoons 2Fe_3O_4 + H_2O \tag{1}$$

$$\text{Magnetite} - \text{iron}\ \ Fe_3O_4 + 4H_2 \leftrightharpoons 3Fe + 4H_2O\ \ T < 843\ \text{K} \tag{2}$$

$$\text{Magnetite} - \text{wustite}\ \ Fe_3O_4 + H_2 \leftrightharpoons 3FeO + H_2O\ \ T > 843\ \text{K} \tag{3}$$

$$\text{Wustite} - \text{iron}\ \ FeO + H_2 \leftrightharpoons Fe + H_2O \tag{4}$$

Whether magnetite reduces directly to Fe (step 2), or via wustite (steps 3 and 4), depends on temperature. The reduction takes place stepwise from Fe_2O_3 to Fe_3O_4 and continues to Fe at the temperature below 843 K. The intermediate oxide FeO is unstable below 843 K; when the temperature rises to 843 K and above, then FeO also be considered in the reduction reaction [8]. With higher temperatures, the stability of FeO increases because of the free spaces in lattices other than iron ions. The thermodynamics of the above four reactions is well explained in the Baur–Glassner diagram, which illustrates the stability of different iron oxide phases as a function of temperature and gas oxidation degree [9]. However, Otsuka and Kunii explained that FeO reduction was marginally increased compared to Fe by using graphite reductant, as the gasification reaction of carbon was influenced by metallic Fe catalyzing [10].

The activation energy was calculated from the plots of the rate of weight loss (at 8% and 19.2%) against the reciprocal of absolute reaction temperature. The activation energy for the initial stages (8% weight loss), at a temperature lower than 873 K, was 42.6 kJ mol^{-1}, and at the higher temperature above 873 K, it was 33.18 kJ mol^{-1}. At a temperature above 873 K, a high value of activation energy was measured in the final stage of reduction, showing solid-state diffusion as the controlling step [11]. Furthermore, the activation energy results achieved by Wang et al. were 68.95 and 82.61 kJ mol^{-1} for hard and soft-coal ore (i.e., high and low volatile content) of Fe pellet; however, El-Geassy et al. conducted the same study in nitrogen (N_2) atmosphere where 18.81 to 28.42 kJ mol^{-1} of activation energy was achieved for non-isothermal

reduction of composite pellets, and during the incubation period. The gaseous diffusion was found dominant for reduction [12].

Later, a comprehensive stage study was conducted by Dutta, on a low heating rate of 10.5 K min^{-1} for the determination of activation energy at different stages of the reduction reaction, where the results showed that during stage I volatile gases diffusion was observed, which resulted in very low activation energy from 6.1 to 13.2 kJ mol^{-1}; in stage II, diffusion of H_2 gas from pores of solid increased the activation energy up to 26.4 to 42.5 kJ mol^{-1}; and during the final stage, due to carbon gasification reaction, the activation energy reached at a maximum level of 183.1 to 268.5 kJ mol^{-1} [13]. This manuscript is a preliminary study of the direct reduction of the iron ores at temperature range from 673 to 1373 K and observation of microstructures during all the stages of the reduction of iron ore particles and pellets using bitumen as a binder.

Methods

Raw material

The first stage in producing a super concentrate (<2% gangue) is to make a high-purity concentrate by a beneficiation process. Subsequently, it can be further upgraded by magnetic separation, flotation, or high-intensity electrostatic separation. Fe_3O_4 has been supplied by L.K.A.B of Sweden, while Fe_2O_3 came from SAMITRI of Brazil. The chemical composition of iron oxides was determined through X-ray fluorescence spectroscopy (XRF) shown in Table 1.

A binding material, 5% bitumen was mixed with Fe_3O_4 and Fe_2O_3 ore in a sigma-bladed mixer at a temperature of 453 K. This bitumen-coated material was compressed using an Avery compression testing machine to produce compact cylindrical pellets (6, 9, and 12 mm). These pellets were baked in an oven at 473 K to gain strength as reported in the previous work of author [11]. High-purity H_2 was used as the reducing agent for both types of pellets. To find the reduction potential of bitumen, Fe_3O_4 and Fe_2O_3 pellets were heated at different temperatures in the N_2 atmosphere.

Table 1 Chemical composition of magnetite and hematite samples

Substance	Composition weight %	
	Magnetite	Hematite
Fe	71.9	69.29
Fe_3O_4	97.0	99.07
Fe_2O_3	2.30	-
SiO_2	0.06	0.35
MgO	0.15	-
Al_2O_3	0.15	0.33
TiO_2	0.14	-
V_2O_5	0.20	-
P	0.004	0.01
Cu	0.005	-
LOI	-	0.24

Direct reduction and analytical measurement

Thermogravimetric analysis (TG) records the continuous measurement of weight change with time in the temperature range of 673 to 1373 K to reduce FeO pellets in the H_2 atmosphere in a Linseis thermogravimetric balance. N_2 gas was flushed through the system for about 7 min before allowing H_2 stream. The sample for the reduction was made up of a 6-mm diameter pellet (approximate 0.5 gm) placed in a mall platinum crucible, and the temperature control unit was set at the reaction temperature and heating rate usually 323 K min^{-1}. After placing the sample into the spoon, the socket was fitted tightly in the cone, ensuring that there was no leakage of gas on flowing through the reaction tube. The hot furnace was then moved over the reaction tube through which H_2 was flowing at the rate of 2.3 l min^{-1} for pellet samples. After completion of a run, the reducing gas was turned off and the reaction tube flushed with N_2. The furnace was switched off and rolled away from the tube to obtain rapid cooling and hence retain the morphological condition of the specimen.

The reaction takes place only on the top surface of the crucible; therefore, the rate should stay constant under the condition of chemical control, but for diffusion control, the rate should decline with time. At high temperatures above 873 K, a fast chemical reaction occurs with the formation of the product layer. As reduction proceeds, the thickness of this layer increases, and thus the rate declines. By assuming that all bitumen has been driven off, the approximate reduction of Fe_3O_4 due to the bitumen can be calculated as [12]:

$$\begin{aligned} Reduction\ (\%) &= \frac{Weight\ loss}{Total\ removable\ oxygen\ present\ in\ the\ sample} \times 100 \\ &= \frac{(W1-W2)}{(W1 \times fore \times \rho ore \times foxygen)} \times 100 \end{aligned}$$

where W1 is the initial weight of the sample, W2 is the final weight of the sample, f ore is a fraction of ore present in a sample = 0.95, ρ ore is a purity of ore, i.e., % of Fe_2O_3 or Fe_3O_4 in ore, f oxygen is a fraction of oxygen present in Fe_2O_3 or Fe_3O_4

Results and discussion

The SEM image in Fig. 1a and b shows that fine Fe_3O_4 ore particles have been agglomerated more effectively than coarser Fe_2O_3 particles (Fig. 1c, d) after mixing with bitumen. Both iron ore agglomerates show good binding capacity with bitumen.

The produced mix was compacted into pellets after cooling to room temperature. The solid particles approach each other closely under the acting pressure, forming a tight connection. The baked pellets, at low temperatures, attained high crushing strength due to the polymerization and hardening of molten bitumen film coating the ore particles. At the point of contact between particles, a solid bridge is formed. Considerably larger bridges are formed when thermoplastic material (such as bitumen) moves under the influence of pressure and friction.

Figure 2a and b of green and baked Fe_3O_4 pellets illustrate the increase in density and improved crushing strength when heated to 400 K, whereas Fig. 2c and d show the green and baked Fe_2O_3 pellets with increased density. At this stage, bitumen well packed with iron oxide polymerizes with the formation of cross-linked polymers.

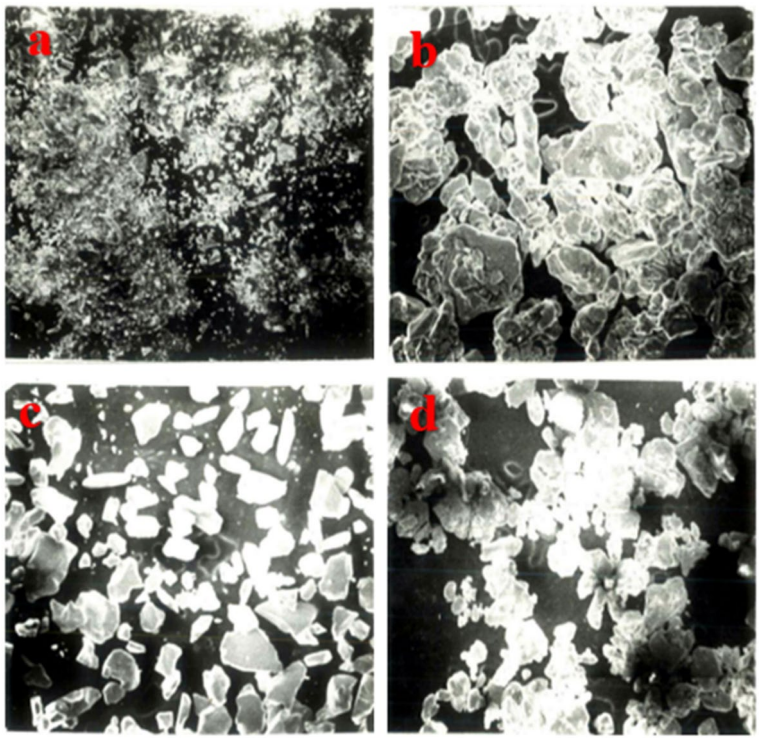

Fig. 1 SEM images (×50) of **a** magnetite particles, **b** magnetite particles with bitumen, **c** hematite particles, and **d** hematite particles with bitumen

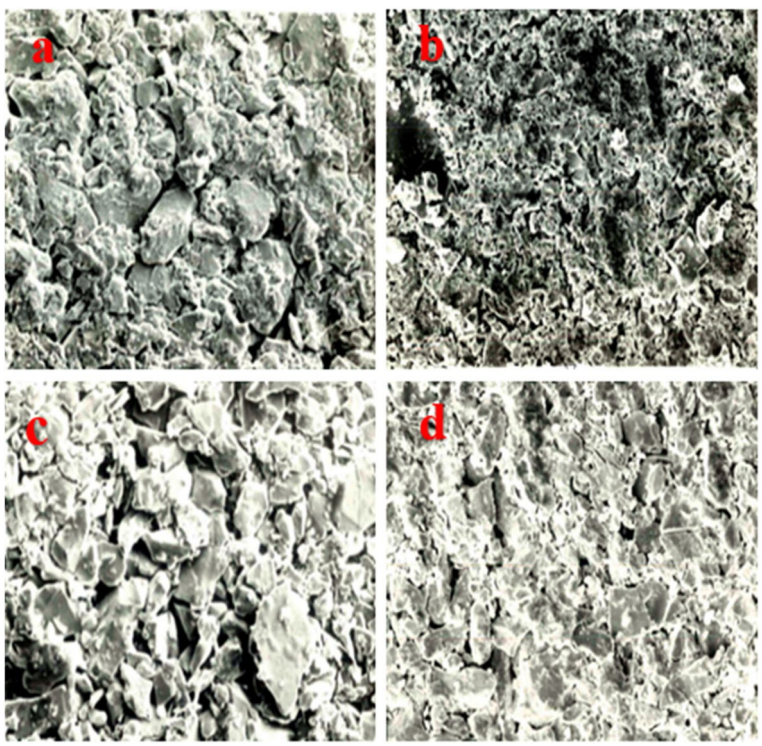

Fig. 2 SEM images (×100) of **a** green magnetite pellet, **b** baked magnetite pellet, **c** green hematite pellet, and **d** baked hematite pellet

Effect of temperature on the microstructures

In the case of Fe_3O_4 super concentrate powder reduced at a lower temperature of 773 K (Fig. 3a), the number of small pores was generated, though the shape of the sample did not change. As the temperature rose to 973 K (Fig. 3b), the particles formed larger pores, but the particles' sharp corners and shape almost remained the same. After a further increase in temperature to 1273 K (Fig. 3c), the sharp corners of the original Fe_3O_4 particles became rounded and smoother, with no open pores visible. This was due to sintering which increased the density of the porous product.

A similar effect for reduced powder of the Fe_2O_3 was observed at different temperatures. At 773 K (Fig. 3d), each grain appeared to be dense. After measuring the pore surface area of the particles, it was concluded that fine pores were present in those dense grains. At 973 K (Fig. 3e), the particles were not as dense as at 773 K, and small pores within some particles can be noticed in Fe_2O_3 particles (×1000) (Fig. 4c) at 973 K. Few cracks are clearly shown in some reduced particles at temperatures 773 K and 973 K respectively in Fig. 3a and b; however, the shape and size of the particle appear to be the same. At 1273 K (Fig. 3f), pores in Fe_2O_3 particles became coarser, but the sharp edges were retained.

Reduced magnetite and hematite with and without 5% bitumen

In Fig. 4, the microstructures of reduced magnetite and hematite particles are compared with 5% bitumen-mixed samples. It can be seen that porosity increased in the case of bitumen-mixed powders of both samples. This was partially due to the evolution of volatiles which leaves behind a highly porous material. The reduction of magnetite powder at 973 K (Fig. 4a) was slower when bitumen was not added. Reduction became faster, and a rate minimum occurred at a higher degree of reduction as compared with magnetite alone. This is another reason why bitumen-added magnetite appears to be more porous

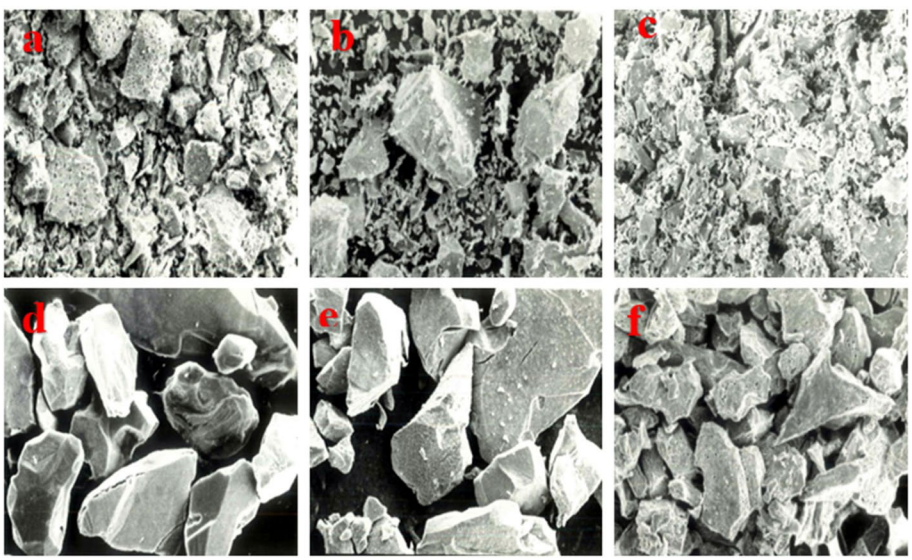

Fig. 3 SEM image (×200) of magnetite particles at **a** 773 K, **b** 973 K, and **c** 1273 K and hematite particles at **d** 773 K, **e** 973 K, and **f** 1273 K

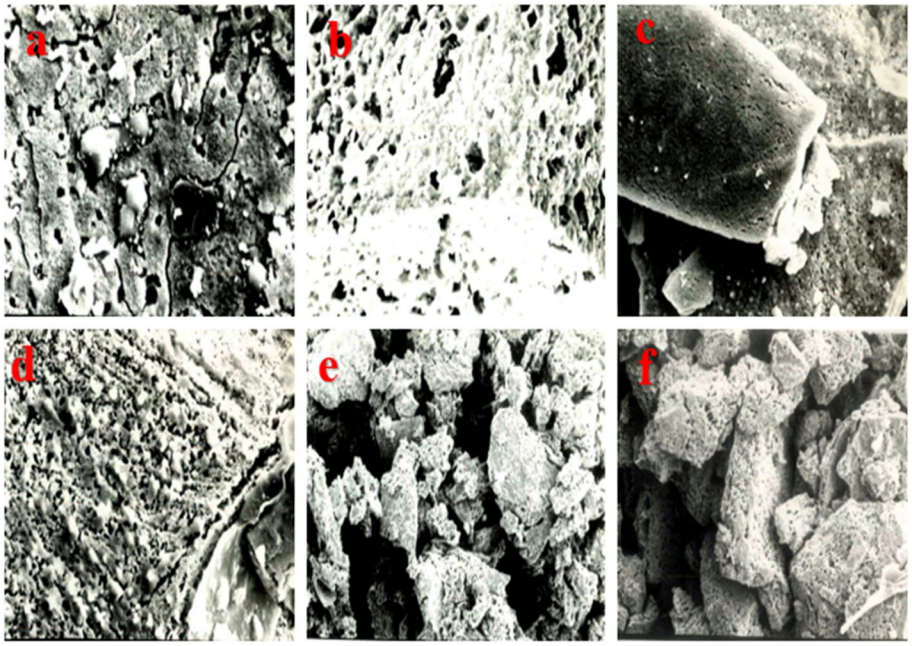

Fig. 4 SEM images (×1000) of **a** magnetite particles at 973 K, **b** magnetite-bitumen mixture at 973 K, **c** hematite particles at 973 K, **d** hematite-bitumen mixture at 973 K, **e** magnetite-bitumen mixture at 1273 K, and **f** hematite-bitumen mixture at 1273 K

as shown in Fig. 4b. Some oxide inclusions were always present in the center of the particles surrounded by cracks as shown in Fig. 4a. Some cracks are also visible in the hematite sample with and without bitumen as shown in Fig. 4c, d.

At high temperatures, such as 1273 K, an additional process occurred during magnetite-bitumen reduction, in which carbon monoxide (CO) was formed, and the reduction rate became faster than when no bitumen was present. This was the effect of high gas pressure build-up within the iron shell resulting in rupture of the shell and exposure of the unreduced oxide to the reducing gas. With H_2 reduction, the gas pressure is not high enough to break the dense iron shell. It is believed that the bursting mechanism would produce a more open structure, and the porosity of iron particles would be increased.

The effect of magnetite-bitumen and hematite-bitumen reduced by H_2 at 1273 K is shown in Fig. 4e and f. Hematite-bitumen specimen (Fig. 4f) is more porous than those with no bitumen (Fig. 3f). The effect of sintering at high magnification is seen in Fig. 4 in case of bitumen-added samples. The pore structure of the specimen shown in Fig. 4e and f with bitumen is coarser than without bitumen (Fig. 3c, f). Turkdogan et al. also found that the pore structure obtained after CO reduction is always coarser than after H_2 reduction [14, 15].

The combustion of organic binders at high temperatures could virtually emit no residual ash to the structure of pellets, leading to slag formation [16]. The softening of bitumen starts at 353 to 363 K; when heated at low (673 K) and high (1273 K) temperatures, the volatiles evolved at 75% and 79% respectively. This volatile reduction was also justified by chemical analysis where fixed carbon was found at 20.5%, and ash content was around 0.12%. Based on this analysis, the bitumen-magnetite mixture

contained 3.96% volatiles and 1.015% fixed carbon. The reduction results for Fe and FeO at high temperatures with hydrocarbon oxidation were found to be extremely favorable, and hydrocarbon volatilization began early in the process, at 573 K, while the oxides were still in the Fe_3O_4 form. H_2 reaction mainly influenced this volatilization, which drives H_2O formation and escaping into the atmosphere [17].

The combustion analysis of blown bitumen showed the chemical percentage for different elements as 82.8% carbon (C), 10% H_2, 4.6% sulfur (S), and 2.7% oxygen (O_2); ash content 0.12%; and 0.5% N_2. During the thermal decomposition of bitumen, the non-condensable gases (H_2, CO, CO_2, H_2S, COS) are also produced with light boiling aromatics. However, under the temperature of 973 K, the formation of carbon and CO_2 from CO is well known. It was observed when the mixture was reduced in the range 673 to 1373 K, the weight loss percentage was much higher than the Fe_3O_4 recorded alone, as shown in Fig. 5a–f.

This difference was mainly caused due to bitumen addition into these powders in the H_2 atmosphere. Figure 5a and b, both showing an increase of 3.7%, is achieved for weight loss after the addition of bitumen. However, the reduction percentage is slightly higher than the total volatile content of the magnetite-bitumen mixture. The results depicted in Fig. 5c–f are considerably interesting, where the increase in weight reduction was slight (1.3%) by increasing temperature up to 873 K as shown in Fig. 5c. This might be because of two possibilities: (I) the maximum reduction of Fe_3O_4 already occurred, and the high diffusion rate of H_2 and water from reacting sample could inhibit the volatilization rate; (II) the deposition reaction of carbon may compatibly occur at a temperature which is thermodynamically favorable which resulted in little increase in weight reduction as achieved on 673 to 773 K. On the contrary, the reduction percentage for 973 to 1073 K as shown in Fig. 5d and e is quite comparably of the same magnitude achieved on 673 to 773 K. However, the reduction was up to 5% when the temperature increased at 1073 K, which indicated that fixed carbon is also participating in the reduction in addition to H_2. Increasing the temperature around 1300 K, the percentage of weight reduction of the mixture was rapid and found larger in magnitude as of the Fe_3O_4 alone. A higher reduction percentage of 9% was found at the initial time of the process.

The results shown in Fig. 5d–f clearly show an increase in weight loss of 5.6%, 9%, and 9.4% at 973 K, 1073 K, and 1373 K respectively. These losses were a combination of the amounts of bitumen and O_2 removed at the respective temperature. It is apparent that after the same time of reduction in H_2, the magnetite-bitumen samples were reduced to higher levels than Fe_3O_4 alone. The increase in reduction rate (above 1073 K) was due to the fixed carbon where gasification increased with temperature, and conversely, the carbon left in the reduced samples decreased. However, H_2 is a fast-reducing agent, and small additions of CO increase after the initial reduction periods at high temperatures.

Conclusions

Overall, the microstructure changes of both Fe_3O_4 and Fe_2O_3 samples were discussed when 5% bitumen was used as a binder at various reduction temperatures in H_2. The Fe_3O_4 super concentrate powder reduced at lower temperatures of 773 K and 973

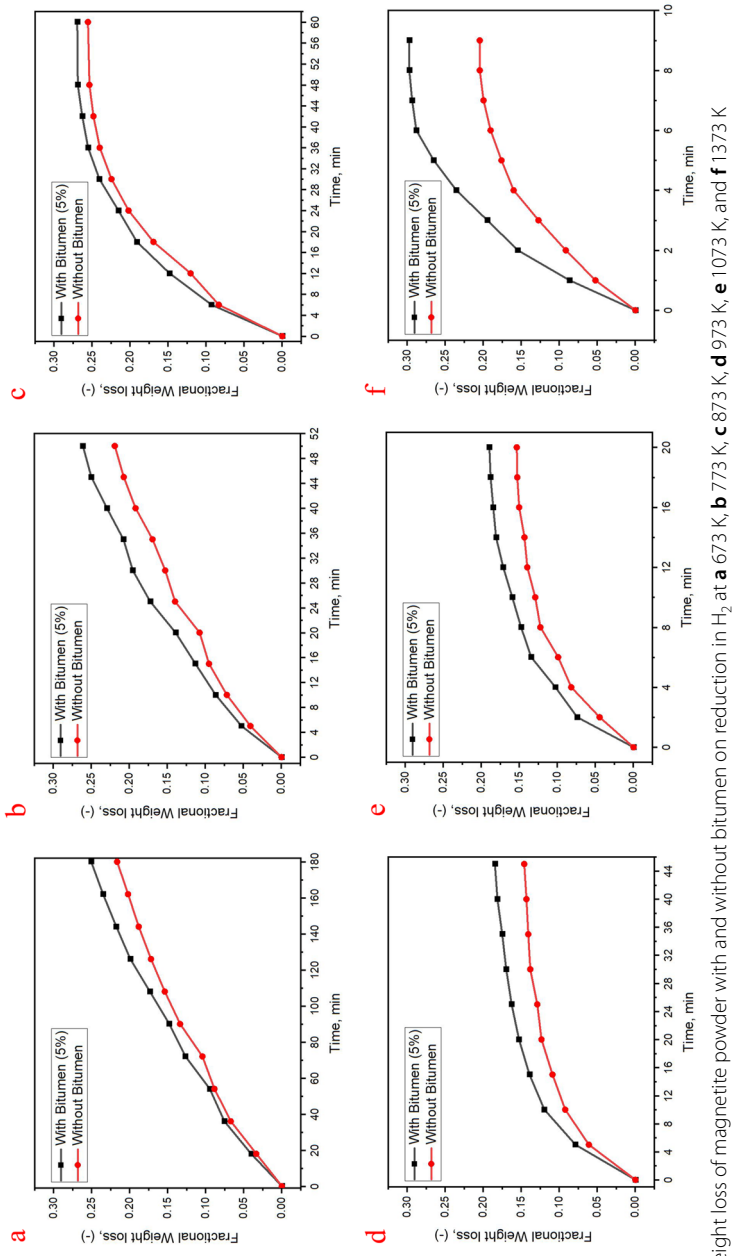

Fig. 5 Comparative weight loss of magnetite powder with and without bitumen on reduction in H_2 at **a** 673 K, **b** 773 K, **c** 873 K, **d** 973 K, **e** 1073 K, and **f** 1373 K

K showed small to larger pores while the particles' sharp corners and general shape retained the same. At a high temperature of 1273 K, the sharp corners of the original Fe_3O_4 particles became rounded and smoother, with no open pores visible. This was due to sintering, which increased the density of the porous product.

The Fe_2O_3 powder appeared to be dense after reduction at 773 K. At 973 K, the particles were not as dense as at 773 K, and small pores within some particles were also visible. In some reduced particles, small cracks can also be seen, at temperatures 773 K and 973 K. At 1273 K, the particle pores became coarser, but the sharp edges were found retained.

The microstructures of reduced Fe_3O_4 and Fe_2O_3 particles, when compared with those which contained 5% bitumen, resulted in increased porosity which was partially due to the evolution of volatiles that leave behind a highly porous material.

Abbreviations

LKAB	Luossavaara-Kiirunavaara Aktiebolag
SAMITRI	SA Mineração da Trindade
TGA	Thermogravimetric analysis
SEM	Scanning electron microscope

Supplementary Information

The online version contains supplementary material available at https://doi.org/10.1186/s44147-022-00137-w.

Additional file 1. 2001-A new manufacturing process of iron and steel.

Acknowledgements
The author would like to thank the courtesy of the British Steel Company and respective institutes.

Authors' contributions
QAK performed experiments and interpreted the results; HL performed the literature survey, wrote the manuscript, and interpreted microstructures; AS contributed in writing; KM generated the reduction curve; and SA contributed in writing and approval of the final manuscript. The authors read and approved the final manuscript.

Funding
Not applicable.

Availability of data and materials
The datasets used and/or analyzed during the current study are available from the corresponding author on reasonable request.

Declarations

Ethics approval and consent to participate
Not applicable.

Consent for publication
Not applicable.

Competing interests
The authors declare that they have no competing interests.

Received: 3 March 2022 Accepted: 24 August 2022
Published online: 07 September 2022

References

1. Yellishetty MM, Gavin M (2014) Substance flow analysis of steel and long term sustainability of iron ore resources in Australia, Brazil, China and India. J Clean Prod 84(1):400–410. https://doi.org/10.1016/j.jclepro.2014.02.046
2. Abhinav B, Mohsen A, Homam NS (2020) Decarbonization of iron and steel industry with direct reduction of iron ore with green hydrogen. energies 13:758. https://doi.org/10.3390/en13030758

3. Zare Ghadi A, Valipour MS, Vahedi SM, Sohn HY (2020) A review on the modeling of gaseous reduction of iron oxide pellets. Steel Res Int 91:1–16. https://doi.org/10.1002/srin.201900270
4. Halt JA, Kawatra SK (2013) Study of organic and inorganic binders on strength of iron oxide pellets. Metallurgical and materials transactions. Miner Metall Process 44(4):1000–1009. https://doi.org/10.1007/s11663-013-9838-4
5. Kotta AB, Patra A, Kumar M, Karak SK (2019) Effect of molasses binder on the physical and mechanical properties of iron ore pellets. Int J Miner Metall Mater 26:41–51. https://doi.org/10.1007/s12613-019-1708-x
6. Ripke SJ, Kawatra SK (2000) Can fly-ash extend bentonite binder for iron ore agglomeration. Int J Miner Process 60(3-4):181–198. https://doi.org/10.1016/S0301-7516(00)00015-6
7. Nikai I, Garbers-Craig AM (2016) Use of iron ore fines in cold-bonded self-reducing composite pellets. Miner Process Extr Metall Rev 37:42–48. https://doi.org/10.1080/08827508.2015.1104506
8. Dabin G, Liandong Z (2016) Direct reduction of oxidized iron ore pellets using biomass syngas as the reducer. Fuel Process Technol 148:276–281. https://doi.org/10.1016/j.fuproc.2016.03.009
9. Spreitzer D, Schenk J (2019) Reduction of iron oxides with hydrogen—a review. Steel Res Int 90. https://doi.org/10.1002/srin.201900108
10. Halder S, Fruehan RJ (2008) Reduction of iron-oxide-carbon composites: part I. estimation of the rate constants. Metall Mater Trans B Process Metall Mater Process Sci 39:784–795. https://doi.org/10.1007/s11663-008-9200-4
11. Ansari AK, Shah SFA et al (2001) A new manufacturing process of iron and steel. J Eng Appl Sci 20:56–63
12. Kemppainen A, Mattila O et al (2012) Effect of H_2–H_2O on the reduction of olivine pellets in CO–CO2 gas. ISIJ Int 52:1973–1978. https://doi.org/10.1021/jp412181f
13. Sah R, Dutta SK (2011) Kinetic studies of iron ore – coal composite pellet reduction by TG – DTA. Trans Indian Inst Metals 64:583–591. https://doi.org/10.1007/s12666-011-0065-x
14. Pal J (2019) Innovative development on agglomeration of iron ore fines and iron oxide wastes. Miner Process Extr Metall Rev 40(4):248–264. https://doi.org/10.1080/08827508.2018.1518222
15. Turkdogan ET (1980) Physical chemistry of high temperature reactions. Academic, New York. https://doi.org/10.1007/s11837-019-03620-7 (Chapter 08)
16. Zhuravlev FM, Lyalyuk VP, Kassim DA et al (2015) Improved iron-ore sinter for blast furnaces. Steel Transl 45:270–274. https://doi.org/10.3103/S0967091215040154
17. Dutta S, Ghosh A (1994) Study of nonisothermal reduction of iron ore-coal/char composite pellet. Metall Mater Trans B Process Metall Mater Process Sci 25:15–26. https://doi.org/10.1007/BF02663174

Publisher's Note